Proceedings of the Sixth International Conference on
Soft Computing, Machine Learning and Optimisation in
Civil, Structural and Environmental Engineering
Edited by: P. Iványi, J. Lógó and B.H.V. Topping
Civil-Comp Conferences, Volume 5, Paper 1.8
Civil-Comp Press, Edinburgh, United Kingdom, 2023
doi: 10.4203/ccc.5.1.8

On design-dependent loads in a NURBS-density-based topology optimisation method

E. Urso, S. Zerrouq, M. Montemurro

Université de Bordeaux, Arts et Métiers Institute of Technology, CNRS, INRA, Bordeaux INP, HESAM Université, I2M UMR 5295, Talence, France

Abstract

This paper deals with topology optimisation (TO) problem with design-dependent loads. Specifically, the problem is formulated in the context of a special density-based TO algorithm wherein a non uniform rational basis spline (NURBS) entity is used to represent the topological descriptor, i.e., the pseudo-density field. In this context, TO problems involving design-dependent loads are addressed, in the most general case of inhomogeneous Neumann-Dirichlet boundary conditions. A study of the penalty function of the design-dependent loads is carried out to investigate its effect on the optimised topologies and overcome the singularity effect related to the zones characterised by low values of the pseudo-density field. Finally, the combination of both design-dependent loads and inhomogeneous Neumann-Dirichlet boundary conditions is investigated and the effectiveness of the method is proven on a 2D benchmark problems.

Keywords: topology optimisation, NURBS surfaces, design-dependent loads, density-based algorithm, inertial loads, penalisation schemes

1 Introduction

Nowadays topology optimisation (TO) is increasingly used in both the academic and the industrial fields thanks to the recent evolution and development of the additive manufacturing technologies that allow the production of different and complex shapes. The aim of TO is to determine the optimal distribution of the material, within a prescribed domain, to minimise a given objective function satisfying a set of design requirements [1]. In the last 30 years, many algorithms for TO have been developed, but among them the two most known and used families of algorithms are represented by the density-based methods [1–4] and the level set method (LSM) [5, 6]. In this paper we focus exclusively on the first class of methods. In density-based TO methods, a penalisation scheme is introduced to avoid meaningless intermediate values of the pseudo-density field and guarantee the convergence to a black and white design. In this context, an efficient and versatile method has been recently developed at the I2M laboratory in Bordeaux ([7–11]) and consists of reformulating the classic density-based algorithms in the framework of non-uniform rational basis spline (NURBS) hyper-surfaces [12–14]. This method, called NURBS-density-based method, introduces different advantages, like the compatibility with computer aided design (CAD) software [8, 15], the independence of the topological descriptor on the finite element (FE) model mesh and, consequently, the reduction of the checker-board effect [13]. It is well known that the most studied problem in the field of TO is that of maximising the structural stiffness under design-independent loads. However, when design-dependent loads are considered, some modifications must be introduced in the problem formulation, as well as in the optimisation process.

When including design-dependent loads in a TO problem, the boundary of the structure evolves during the optimisation process and consequently, the design-dependent loads change their locations, magnitudes and/or directions as the TO analysis progresses [16]. Accordingly, this class of problems is characterised by three main issues: the non-monotonous behaviour of the compliance, the inactive volume constraint of the optimal topology and the low density parasitic effects when using classical penalisation schemes, like the SIMP one [16, 17].

This work aims to investigate this class of TO problems in presence of inertial loads in the framework of the NURBS-density-based method. Firstly, the expression of the gradient of the merit function, i.e., the generalised compliance [10], is provided in the most general case of inhomogeneous Neumann-Dirichlet boundary conditions (BCs). Successively, different penalisation schemes are studied to overcome the drawbacks associated with design-dependent loads and a new penalisation scheme is proposed to deal with the issues mentioned above. Numerical tests are conducted on a meaningful 2D benchmark problem to investigate all the aspects mentioned above.

The remainder of the paper is as follows. The fundamentals of the NURBS density-based method are recalled in Section 2. The penalisation schemes used in this work are introduced in Section 3. The numerical analyses aimed at investigating the influence of the non-zero Neumann-Dirichlet boundary condition and the penalty schemes on

the optimised designs are presented in Section 4. Finally, Section 5 ends the paper with some concluding remarks and prospects.

2 The NURBS-density-based method

The NURBS-density-based method is briefly described for 2D TO problems in the following. For more details the reader is addressed to [7, 10, 18]. Without loss of generality, in the following the design domain is defined as a compact rectangular of size $L_1 \times L_2$. Of course, the size and shape of the 2D design domain can be different but can be always embedded in a rectangle. Thus, let $\mathcal{D} := \{(x_1, x_2) \in \mathbb{R}^2 \mid x_j \in [0, L_j],\ j = 1, 2.\}$ be a compact subset defined in the Cartesian orthogonal frame $\mathcal{O}(x_1, x_2)$ representing the design domain. In the framework of the NURBS-density-based method, the topological variable, i.e., the pseudo-density field, for a 2D problem is represented through a 3D surface, where the first two coordinates represent the Cartesian coordinates, while the last one is the pseudo-density field, which reads:

$$\rho(\zeta_1, \zeta_2) = \sum_{\mathrm{i}_1=0}^{n_1} \sum_{\mathrm{i}_2=0}^{n_2} R_{\mathrm{i}_1\mathrm{i}_2}(\zeta_1, \zeta_2)\rho_{\mathrm{i}_1\mathrm{i}_2}. \tag{1}$$

In Eq. (1), $\rho_{i_1 i_2}$ is the value of the pseudo-density at the generic control point (CP) of the NURBS surface, $\zeta_k \in [0,\ 1]$ is the k-th parametric coordinate, and $(n_k + 1)$ is the number of CPs along this direction. The total number of CPs is $n_{\mathrm{CP}} := \prod_{i=1}^{2}(n_i + 1)$, while $R_{i_1 i_2}$ is rational basis function defined as: The rational basis function $R_{i_1 i_2}$ in Eq. (1) is defined as:

$$R_{i_1 i_2} := \frac{\omega_{i_1 i_2} \prod_{k=1}^{2} N_{i_k, p_k}(\zeta_k)}{\sum_{j_1=0}^{n_1} \sum_{j_2=0}^{n_2} \left[\omega_{j_1 j_2} \prod_{k=1}^{2} N_{j_k, p_k}(\zeta_k)\right]}, \tag{2}$$

where $N_{i_k, p_k}(\zeta_k)$ are the Bernstein's polynomials of degree p_k [13] and $\omega_{i_1 i_2}$ is the weight associated with the generic CP whose value influences the way the surface is attracted towards that CP. The dimensionless parameters ζ_j can be defined as:

$$\zeta_j = \frac{x_j}{L_j}, \quad j = 1, 2, \tag{3}$$

where x_j is the Cartesian coordinate along the j-th axis defining the design domain and L_j is the characteristic length defined along that axis. The shape of the NURBS surface is affected by different parameters, of which only the pseudo-density values at the CPs and the associated weights are considered as *design variables* and arranged in the arrays $\boldsymbol{\xi}_1 \in \mathbb{R}^{n_{\mathrm{CP}} \times 1}$ and $\boldsymbol{\xi}_2 \in \mathbb{R}^{n_{\mathrm{CP}} \times 1}$:

$$\boldsymbol{\xi}_1^T := \{\rho_{00}, ..., \rho_{\mathrm{n}_1\mathrm{n}_2}\},\ \boldsymbol{\xi}_2^T := \{\omega_{00}, ..., \omega_{\mathrm{n}_1\mathrm{n}_2}\},\ \boldsymbol{\xi}_1, \boldsymbol{\xi}_2 \in \mathbb{R}^{n_{\mathrm{CP}}}. \tag{4}$$

According to Eq. (4), the number of design variables is at most $n_{\mathrm{var}} = 2n_{\mathrm{CP}}$ in the case of NURBS. In the framework of the NURBS-density-based method, the derivation of the formal expression of the gradient of the physical requirements is facilitated

by the use of the local support property of the Bernstein's polynomials [10, 13] and exploiting the chain rule. When design-dependent loads are applied to the structure in the general case of non-zero Neumann-Dirichlet boundary conditions [10], the governing equation of the static equilibrium problem reads:

$$\begin{bmatrix} \mathbf{K} & \mathbf{K}_{\mathrm{BC}} \\ \mathbf{K}_{\mathrm{BC}}^{\mathbf{T}} & \tilde{\mathbf{K}} \end{bmatrix} \begin{Bmatrix} \mathbf{u} \\ \mathbf{u}_{\mathrm{BC}} \end{Bmatrix} = \begin{Bmatrix} \mathbf{f} \\ \mathbf{r} \end{Bmatrix}, \tag{5}$$

where $\mathbf{u}$ and $\mathbf{u}_{\mathrm{BC}}$ are the unknown and imposed vectors of generalised displacements respectively, $\mathbf{K}$, $\mathbf{K}_{\mathrm{BC}}$ and $\tilde{\mathbf{K}}$ are the stiffness matrices of the FE model after applying the BCs. The vector $\mathbf{r}$ contains the nodal reactions and depends on the imposed BCs, while the vector of external forces $\mathbf{f}$ depends upon the density field, i.e., $\mathbf{f} = \mathbf{f}_0 + \mathbf{f}_i\left(\rho\left(\mathbf{x}\right)\right)$, $\mathbf{f}_0$ and $\mathbf{f}_i$ being the design-independent and inertial forces, respectively. The equilibrium, in its compact form, is written as:

$$\hat{\mathbf{K}}\hat{\mathbf{u}} = \hat{\mathbf{f}}. \tag{6}$$

The generalised compliance, introduced as cost function by Montemurro [10], reads:

$$\mathcal{C} = \mathbf{f}^{\mathbf{T}}\mathbf{u} - \mathbf{u}_{\mathrm{BC}}^{\mathbf{T}}\mathbf{r}, \tag{7}$$

while its partial derivatives, in presence of a design-dependent loads, become:

$$\frac{\partial \mathcal{C}}{\partial \xi_{i\tau}} = \sum_{\mathrm{e}\in\mathcal{S}_\tau} \frac{\partial \rho_e}{\partial \xi_{i\tau}} \left(\frac{2w_{\mathrm{e,ext}}}{\phi_{fe}} \frac{\partial \phi_{fe}}{\partial \rho_e} - \frac{w_{\mathrm{e}}}{\phi_{Ke}} \frac{\partial \phi_{Ke}}{\partial \rho_e} \right), \; i = 1, 2 \; \tau = 1, \ldots, n_{\mathrm{CP}}, \tag{8}$$

where ϕ_{fe} and ϕ_{Ke} are the functions used to penalise the inertial loads and the stiffness matrix, respectively, evaluated at the element centroid (see Section 3 for more details), while the term $\dfrac{\partial \rho_e}{\partial \xi_{i\tau}}$ is the partial derivative of the NURBS surface that can be found in [10]. Unlike the formulation presented in [10], a new term occurs in the evaluation of the compliance gradient related to the presence of design-dependent loads. Particularly, in Eq. (8), $w_{e,\mathrm{ext}}$ is the work of the design-dependent loads applied to the nodes of the generic element, whilst w_e is the internal work (which is twice the strain energy of the element). Consider, now, the case of the self-weight as inertial load. It can be expressed as:

$$\mathbf{f}_{ie}^{0} = \frac{1}{4} \varrho_{me} V_e g \boldsymbol{\iota}_0, \tag{9}$$

where V_e and ϱ_{me} are the volume and the density of the material of the generic element, respectively, while g is the gravitational acceleration. The vector $\boldsymbol{\iota}_0$ depends on the type and shape of the generic element. For a quadrilateral element with four nodes and two degrees of freedom (DOFs) per node, it is defined as:

$$\boldsymbol{\iota}_{0i}^{\mathrm{T}} = \left(0, -1, 0, -1, 0, -1, 0, -1\right). \tag{10}$$

The design requirement considered in this study is about the lightness and is expressed through a constraint on the volume of the structure. The associated constraint function reads:

$$g(\boldsymbol{\xi}_1, \boldsymbol{\xi}_2) := \frac{V}{V_{\mathrm{ref}}} - \gamma = 0, \tag{11}$$

where V_{ref} is a reference value of the volume and γ is the prescribed volume fraction. Therefore, the problem is formulated as a constrained non-linear programming problem (CNLPP) as follows:

$$\min_{\boldsymbol{\xi}_1,\boldsymbol{\xi}_2} \frac{\mathcal{C}(\boldsymbol{\xi}_1,\boldsymbol{\xi}_2)}{|\mathcal{C}_{\text{ref}}|} \text{ , subject to: } \begin{cases} \hat{\mathbf{K}}\hat{\mathbf{u}} = \hat{\mathbf{f}}, \\ g(\boldsymbol{\xi}_1,\boldsymbol{\xi}_2) = 0, \\ \boldsymbol{\xi}_{1\text{j}} \in [\rho_{\min},\rho_{\max}],\ \boldsymbol{\xi}_{2\text{j}} \in [\omega_{\min},\omega_{\max}], \\ j = 1,...,n_{\text{CP}}, \end{cases} \tag{12}$$

where $\mathcal{C}_{\text{ref}}$ is the reference value of the compliance of the structure (the absolute value is considered in the above formula because in the case of non-zero mixed BCs the compliance is not a positive definite function), $\rho_{\min}$ and $\rho_{\max}$ are lower and upper bounds for the pseudo-density evaluated at each CP, while $\omega_{\min}$ and $\omega_{\max}$ are the bounds for the weights. To avoid singularity the lower bound of the pseudo-density must be strictly positive. In all the analyses carried out in this paper, the bounds of the design variables have been set as follows: $\rho_{\min} = 0.001$, $\rho_{\max} = 1.0$, $\omega_{\min} = 0.5$, $\omega_{\max} = 10.0$.

3 The penalisation schemes

The choice of the material interpolation scheme constitutes an important step of the problem definition: it influences the optimal topology, the convergence of the problem and can affect the problem through parasitic effects and singularity issues [17, 19]. However, choosing a proper penalisation scheme is anything but trivial. The schemes used in this study are briefly discussed below.

3.1 Penalisation of the inertial loads

The inertial loads of the generic element e are penalised according to the following formula:

$$\mathbf{f}_{ie} = \phi_{fe}\mathbf{f}^0_{ie}, \tag{13}$$

where the expression of $\mathbf{f}^0_{ie}$ is given in Eq. (9) in the case of the self-weight. In this paper, two different types of penalisation function ϕ_f are considered. The first and easier penalisation scheme that one can formulate is a linear penalisation scheme that reads:

$$\phi_f(\rho_e) = \rho_e, \quad \frac{\partial\phi_f(\rho_e)}{\partial\rho_e} = 1. \tag{14}$$

The second one is a modified version of the linear penalisation scheme, which reads:

$$\phi_f(\rho_e) = \left(\frac{\rho_e - \rho_{\min}}{1-\rho_{\min}}\right)^{\beta}, \ \frac{\partial\phi_f(\rho_e)}{\partial\rho_e} = \frac{\beta}{1-\rho_{\min}}\left(\frac{\rho_e - \rho_{\min}}{1-\rho_{\min}}\right)^{\beta-1}. \tag{15}$$

This second scheme has been introduced to avoid singularity of the solution of the equilibrium problem (in terms of the displacement field) when the pseudo-density

takes low values [17]. Indeed, when using the linear penalisation law for the inertial forces and the SIMP scheme for the element stiffness matrix, when $\rho_e = \rho_{\min}$ this would result in a set of inertial loads having a finite value applied to an element with a near-zero stiffness matrix. Conversely, using the penalty scheme of Eq. (15), when $\rho_e = \rho_{\min}$ the inertial loads are exactly zero, regardless of the penalisation scheme used for the stiffness matrix. For the numerical analyses presented in this paper, the parameter β has been set equal to one.

3.2 Penalisation of the stiffness matrix

The stiffness matrix of the generic element e is penalised as follows:

$$\mathbf{K}_e = \phi_{Ke}\mathbf{K}_e^0, \tag{16}$$

where $\mathbf{K}_e^0$ is the unpenalised stiffness matrix, whose expression is given in [10]. In this paper, three different types of penalisation functions ϕ_K are considered. The polynomial penalisation law used [20] reads:

$$\phi_K(\rho_e) = (1-\varepsilon)\rho_e^\alpha + \varepsilon\rho_e, \quad \frac{\partial\phi_K(\rho_e)}{\partial\rho_e} = \alpha(1-\varepsilon)\rho_e^{\alpha-1} + \varepsilon, \tag{17}$$

where $\alpha > 1$ is the penalisation parameter (in this work $\alpha = 3$ is considered), while the parameter $\varepsilon = \frac{1}{16}$ is introduced to avoid that, for small values of density, a mismatch finite-infinite occurs. The second penalty scheme is the Rational Approximation of Material properties (RAMP) [21], which has the advantage that the partial derivative takes a finite value when the pseudo-density goes to zero, achieving better performance for TO problems with design-dependent loads. The RAMP scheme can be expressed as:

$$\phi_K(\rho_e) = \frac{\rho_e}{1+q(1-\rho_e)}, \quad \frac{\partial\phi_K(\rho_e)}{\partial\rho_e} = \frac{1+q}{\left[1+q\left(1-\rho_e\right)\right]^2}, \tag{18}$$

where q is the penalisation parameter and it is usually set as $q = 8$ to penalise intermediate values of the pseudo-density field. The third penalisation scheme is the SIMP approach [1, 2, 22], which reads:

$$\phi_K(\rho_e) = \rho_e^\alpha, \quad \frac{\partial\phi_K(\rho_e)}{\partial\rho_e} = \alpha\rho_e^{\alpha-1}, \tag{19}$$

where α is the penalty parameter: which has been set as $\alpha = 3$.

4 Numerical results

Numerical analyses are performed to test the effectiveness of the proposed method and evaluate the combined effects of design-dependent loads and inhomogeneous

Penalisation scheme	DC1	DC2	DC3	DC4
Inertial load	Eq. (14)	Eq. (14)	Eq. (15)	Eq. (15)
Stiffness matrix	Eq. (18)	Eq. (17)	Eq. (19)	Eq. (18)

Table 1: Design cases.

Neumann-Dirichlet boundary conditions. The method is implemented in SANTO (SIMP and NURBS for topology optimisation), developed in [9, 11] and coded in Python. The 2D benchmark, taken from [17], is shown in Fig 1 and it is characterised by the following geometrical parameters: $L_1 = 200$ mm, $L_2 = 100$ mm and thickness $t = 1$ mm. The FE model is constituted of $N_e = 40 \times 80$ PLANE182 elements (plane elements characterised by four nodes with two DOFs for each one and plane stress hypothesis) and it is obtained through the software ANSYS APDL. A zero dis-

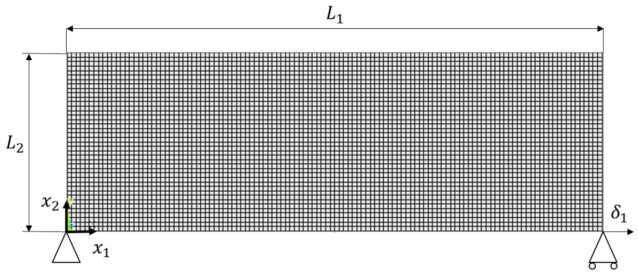

Figure 1: 2D benchmark subjected to design-dependent loads and inhomogeneous Neumann-Dirichlet BCs.

placement is set at the node $(x_1, x_2) = (0, 0)$, while on the node $(x_1, x_2) = (L_1, 0)$, the displacement $u_2 = 0$ is imposed. Moreover, a gravitational load is applied on the whole body, imposing $g = 9.8066$ m/s^2 as gravitational acceleration along the y-axis and a variable horizontal displacement δ_1 is imposed on the node located at $(x_1, x_2) = (L_1, 0)$, assuming the values $\delta_1 \in \{-10, -7, -4, -1, 0, 1, 4, 7, 10\} \times 10^{-3}$ mm for each case considered. The material properties used for this benchmark are: $E = 2e5$ MPa, $\nu = 0.3$ and $\varrho_m = 7.85e-6$ kgmm^{-3}. The numerical simulations are carried out considering a NURBS surface as a descriptor of the pseudo-density field with a degree $p = 3$. The number of CPs is equal to $N_{\text{CP}} = \frac{3}{4}N_e = 75 \times 32$. These parameters have been chosen as a results of a sensitivity analysis that is not illustrated here for the sake of brevity, but that will be shown during the speech. The analyses presented in this section are carried out considering a volume fraction $\gamma = 0.4$ and for four design cases (DC) corresponding to just as many penalisation schemes combinations as listed in Table **??**. The CNLPP of Eq. (12) has been solved with the globally convergent method of moving asymptotes (GC-MMA) algorithm [23] with the parameters presented in [10]. The results are shown in Figs. 2-5 in terms of generalised compliance vs. the applied displacement for the different DCs described above. For each optimised topology, the number of iterations to achieve convergence is also given in each plot. Moreover, the constraint on the volume fraction is met for

each optimised design. From the analysis of these results, one can notice that when considering DC3, the optimisation process achieves the convergence in less iterations, except for the case $\delta_1 = 0$ mm where the solution search process probably stucks in a saddle point (characterised by intermediate values of the pseudo-density field). It is noteworthy that all the penalisation schemes lead to the same trend of the generalised compliance vs. the imposed displacement, with negatives values for all the values of δ_1 (except the case $\delta_1 = 0$) and lower values of the objective function for DC3 and DC4. In contrast, DC2 and DC3 bring to similar optimal topologies, while DC1 and DC4 lead to solution similar to each other but substantially different from the other two DCs.

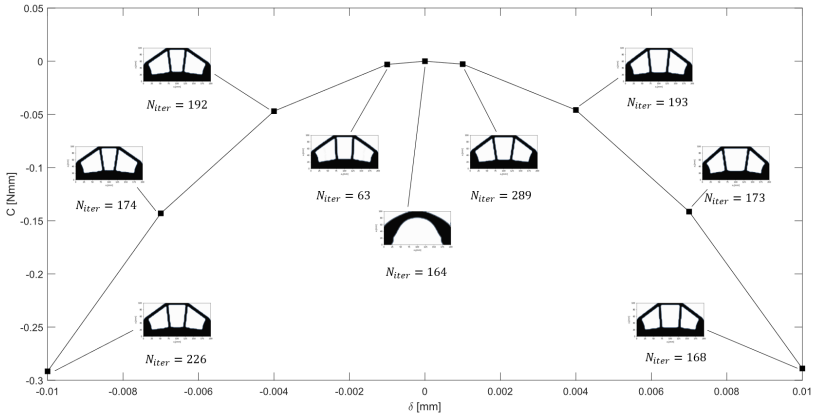

Figure 2: Optimised solutions of the 2D benchmark subjected to design-dependent load and mixed non-zero BCs: DC1.

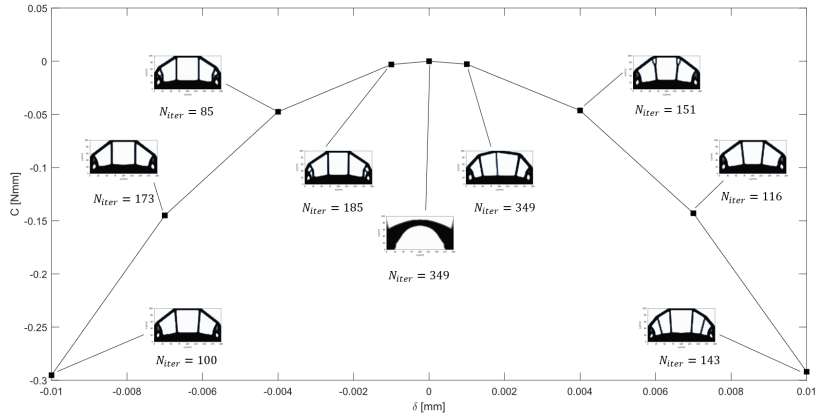

Figure 3: Optimised solutions of the 2D benchmark subjected to design-dependent load and mixed non-zero BCs: DC2.

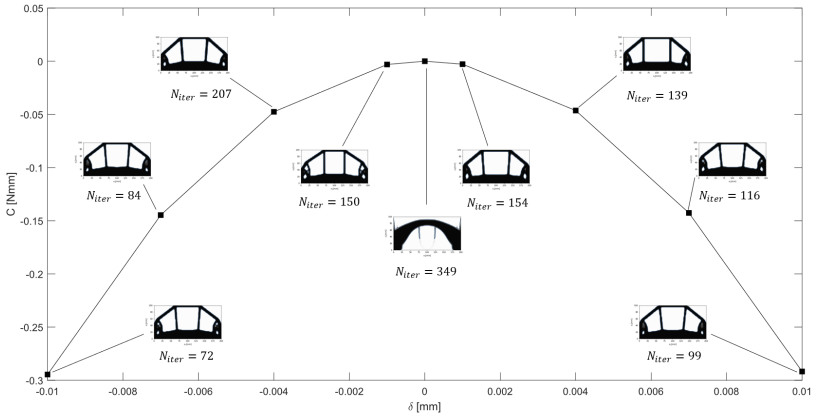

Figure 4: Optimised solutions of the 2D benchmark subjected to design-dependent load and mixed non-zero BCs: DC3.

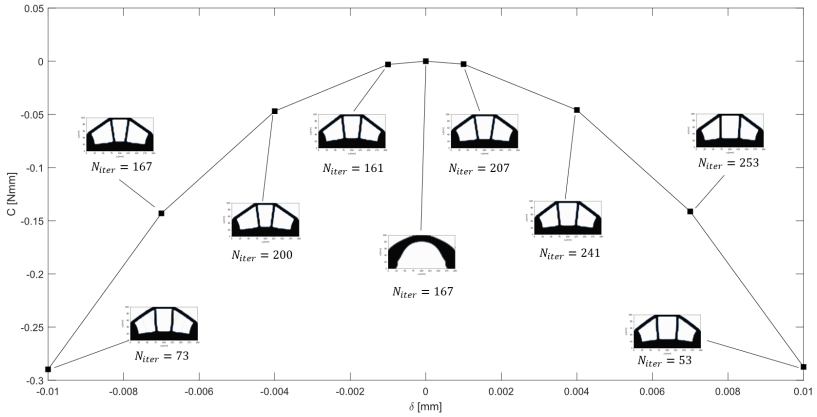

Figure 5: Optimised solutions of the 2D benchmark subjected to design-dependent load and mixed non-zero BCs: DC4.

5 Concluding remarks

In this paper, TO problems involving design-dependent loads have been reformulated and studied in the framework of the NURBS-density-based TO algorithm. The analysis has been limited to the case of inertial forces.

Specifically, the influence of different penalty schemes on the optimised topology is investigated by considering different combinations of penalty functions for both inertial loads and stiffness matrix. It is noteworthy from the obtained results that all the penalisation schemes lead to the same trend of merit function vs. applied displacement, with negative values for all the non-null displacements. Moreover, the optimisation process considering DC3 achieves the convergence in less iterations, except for the case $\delta_1 = 0$ mm, which constitutes a saddle point of the TO problem. Globally, the lower values of the objective function are achieved for DC3 and DC4.

Further analyses on 2D and 3D benchmark structures will be illustrated during the presentation.

Regarding the prospects of this study, research is ongoing to extend the proposed approach to different kind of design-dependent loads, e.g., thermomechanical loads.

Acknowledgements

E. Urso is grateful to SAFRAN Helicopter Engines for supporting this work through the funding of her internship. S. Zerrouq and M. Montemurro are grateful to French National Research Agency for supporting this work through the research project GLAMOUR-VSC ANR-21-CE10-0014.

References

[1] M. P. Bendsoe, O. Sigmund, Topology Optimization: Theory, Methods, and Applications. Dec. 1, 2003.

[2] M. P. Bendsøe, N. Kikuchi, "Generating optimal topologies in structural design using a homogenization method," Computer Methods in Applied Mechanics and Engineering, Nov. 1, 1988. DOI: 10.1016/0045-7825(88)90086-2.

[3] O. Sigmund, "A 99 line topology optimization code written in Matlab," Structural and Multidisciplinary Optimization, Apr. 1, 2001. DOI: 10.1007/s001580050176.

[4] O. Sigmund, "Morphology-based black and white filters for topology optimization," Structural and Multidisciplinary Optimization, Apr. 1, 2007. DOI: 10.1007/s00158-006-0087-x.

[5] G. Allaire, F. Jouve, A.M. Toader, "Structural optimization using sensitivity analysis and a level-set method," Journal of Computational Physics, Feb. 2004. DOI: 10.1016/j.jcp.2003.09.032.

[6] G. Allaire, F. Jouve, "A level-set method for vibration and multiple loads structural optimization," Computer Methods in Applied Mechanics and Engineering, Aug. 12, 2005. DOI: 10.1016/j.cma.2004.12.018.

[7] G. Costa, M. Montemurro, J. Pailhes, "A 2d topology optimisation algorithm in NURBS framework with geometric constraints," International Journal of Mechanics and Materials in Design, Dec. 1, 2018. DOI: 10 . 1007/s10999-017-9396-z.

[8] G. Costa, M. Montemurro, J. Pailhes, "A general hybrid optimization strategy for curve fitting in the non-uniform rational basis spline framework," Journal of Optimization Theory and Applications, Jan. 2018. DOI: 10.1007/s10957-017-1192-2.

[9] G. Costa, M. Montemurro, J. Pailhes, "NURBS hyper-surfaces for 3d topology optimization problems," Mechanics of Advanced Materials and Structures, May 16, 2019. DOI: 10.1080/15376494.2019.1582826.

[10] M. Montemurro, "On the structural stiffness maximisation of anisotropic continua under inhomogeneous neumann-dirichlet boundary conditions," Composite Structures, DOI: 10.1016/j.compstruct.2022.115289.
[11] G. Costa, "Design and optimisation methods for structures produced by means of additive layer manufacturing processes," These de doctorat, Paris, ENSAM, Oct. 2018.
[12] P. Bezier, Courbes et surfaces,Paris, 1986.
[13] W. T. L. Piegl, The NURBS Book, Berlin, 1995, DOI: 10.1007/978-3-642-97385-7.
[14] G. E. Farin, Curves and surfaces for CAGD: a practical guide (Morgan Kaufmann series in computer graphics and geometric modeling), 5th ed. San Francisco, CA: Morgan Kaufmann, 2001.
[15] G. Bertolino, G. Costa, M. Montemurro, N. Perry, F. Pourroy, A general surface reconstruction method for post-processing of topology optimisation results, Sep. 13, 2019.
[16] P. Kumar, M. Langelaar, "On topology optimization of design-dependent pressure-loaded three-dimensional structures and compliant mechanisms," International Journal for Numerical Methods in Engineering, vol. 122, 2021. DOI: 10.1002/nme.6618.
[17] M. Bruyneel, P. Duysinx, "Note on topology optimization of continuum structures including self weight," Structural and Multidisciplinary Optimization, Apr. 2005. DOI: 10.1007/s00158-004-0484-y.
[18] G. Costa, M. Montemurro, J. Pailhes, "Minimum length scale control in a NURBS-based SIMP method," Computer Methods in Applied Mechanics and Engineering, Sep. 1, 2019. DOI: 10.1016/j.cma.2019.05.026.
[19] J. Deaton, R. Grandhi, Topology Optimization of Thermal Structures with Stress Constraints, Apr. 8, 2013. DOI: 10.2514/6.2013-1466.
[20] J. Baroth, P. Bressolette, C. Chauviere, M. Fogli, "An efficient SFE method using lagrange polynomials: Application to nonlinear mechanical problems with uncertain parameters," Computer Methods in Applied Mechanics and Engineering, Sep. 2007. DOI: 10.1016/j.cma.2007.04.017.
[21] K. Stolpe, M. Svanberg, "An alternative interpolation scheme for minimum compliance topology optimization," Structural and Multidisciplinary Optimization, Sep. 1, 2001. DOI: 10.1007/s00158010012.
[22] H. A. Eschenauer, N. Olhoff, "Topology optimization of continuum structures: A review," Applied Mechanics Reviews, Jul. 1, 2001. DOI: 10.1115/1.1388075.
[23] K. Svanberg, "A class of globally convergent optimization methods based on conservative convex separable approximations," SIAM Journal on Optimization, Jan. 2002. DOI: 10.1137/S1052623499362822.